LBL-24651
Preprint

Lawrence Berkeley Laboratory
UNIVERSITY OF CALIFORNIA

RECEIVED
LAWRENCE
BERKELEY LABORATORY

JUL 27 1988

LIBRARY AND
DOCUMENTS SECTION

Submitted to Revue Roumaine de Physique

Systematics of Target Fragment Mass Distributions in Intermediate and High Energy Nuclear Collisions

W. Loveland and G.T. Seaborg

December 1987

TWO-WEEK LOAN COPY
This is a Library Circulating Copy
which may be borrowed for two weeks.

NUCLEAR SCIENCE DIVISION

LBL-24651

Prepared for the U.S. Department of Energy under Contract Number DE-AC03-76SF00098.

DISCLAIMER

This document was prepared as an account of work sponsored by the United States Government. While this document is believed to contain correct information, neither the United States Government nor any agency thereof, nor the Regents of the University of California, nor any of their employees, makes any warranty, express or implied, or assumes any legal responsibility for the accuracy, completeness, or usefulness of any information, apparatus, product, or process disclosed, or represents that its use would not infringe privately owned rights. Reference herein to any specific commercial product, process, or service by its trade name, trademark, manufacturer, or otherwise, does not necessarily constitute or imply its endorsement, recommendation, or favoring by the United States Government or any agency thereof, or the Regents of the University of California. The views and opinions of authors expressed herein do not necessarily state or reflect those of the United States Government or any agency thereof or the Regents of the University of California.

SYSTEMATICS OF TARGET FRAGMENT MASS DISTRIBUTIONS IN INTERMEDIATE AND HIGH ENERGY NUCLEAR COLLISIONS

Submitted to Revue Roumaine de Physique for a special issue
dedicated to Professor Ioan Ursu on the occasion of
his 60th birthday

Walter Loveland

Department of Chemistry
Oregon State University
Corvallis, Oregon 97331

and

Glenn T. Seaborg

Nuclear Science Division
Lawrence Berkeley Laboratory
University of California
Berkeley, Californa 94720

December 1987

This work was supported by the Director, Office of Energy Research, Division of Nuclear Physics of the Office of High Energy and Nuclear Physics of the U.S. Department of Energy under Contract DE-AC03-76SF00098.

SYSTEMATICS OF TARGET FRAGMENT MASS DISTRIBUTIONS IN INTERMEDIATE AND HIGH ENERGY NUCLEAR COLLISIONS

W. LOVELAND[a] and G. T. SEABORG[b]

[a]Dept. of Chemistry,
Oregon State University
Corvallis, OR 97331

[b]Nuclear Science Division,
Lawrence Berkeley Laboratory,
University of California
Berkeley, CA 94720

Dedicated to Professor I. Ursu on the occasion of his 60th birthday

Abstract:

A summary of the target fragment mass distributions from the interaction of 8.5 - 14,500 MeV/nucleon lighter heavy ions (C - Ne) with targets ranging from Cu to U is presented. The measured distributions are compared with predictions of the intranuclear cascade model as well as semi-empirical prescriptions to describe fragment yields.

1. Introduction

For over ten years, nuclear chemists have measured the target fragment isobaric yield distributions from relativistic ($E_{proj} \geq 250$ MeV/nucleon) nucleus-nucleus collisions. For over five years, similar measurements have been made for intermediate ($E_{proj} \leq 100$ MeV/nucleon) energy nuclear collisions. In this paper, we summarize the results of these measurements and compare them to relevant semi-classical models of nucleus-nucleus collisions. In doing so, we hope that the data will serve as guides to more sophisticated measurements of these reactions and as suitable benchmarks for calculations of the various reaction mechanism(s) involved. The data may also be of interest to those who study cosmic ray interactions with matter.

2. Results

A representative sample of the data on target fragment isobaric yield distributions for the interaction of lighter heavy ions (C - Ne) with Cu, Ho, Au and U is shown in Figures 1-7. Wherever possible we have shown the individual fragment isobaric yields (which are uncertain to $\sim\pm40\%$). Where this was not feasible, a smooth curve was fitted to the measured yields. Additional data for the fragmentation of Ag[15,16], Sm[9,17] and Ta[6,18] exist. Qualitatively, one observes the fragmentation of U to be dominated by fission de-excitation of most fragments produced in the initial nucleus-nucleus collision. Spallation-like processes contribute to the yields of fragments with $A > 70$[19] and multifragmentation results in products with $A < 60$. For Au target fragmentation one observes complete fusion processes at the lowest projectile energies resulting in evaporation residues and fission fragments. As the projectile energy is raised incomplete fusion processes become increasingly important until about 35 MeV/nucleon

where complete fusion processes are negligible.[20] Further increases in projectile energy result in increasing spallation and fragmentation processes with Au and with Ho, fission decreases as a fragment de-excitation mechanism as the projectile energy increases. In the case of a nucleus like Ho which only fissions when it is made to rotate rapidly, the decrease in fission cross section with increasing projectile energy can be linked directly to the decrease in the angular momentum of the fissioning system[21]. From $35 \leq A \leq 55$, the fragment yields from Cu fragmentation decrease roughly exponentially with decreasing fragment mass. The slope of these mass yield curves is greatest for the lowest energies and is least for the highest projectile energies, presumably reflecting the increase in the yields of lower A fragments with increasing projectile (excitation) energy resulting in more particle evaporation.

3. Semi-empirical models

There have been a number of attempts to describe the fragment mass distributions from high energy nuclear collisions in terms of semi-empirical models. One of the potentially most powerful of these models is the universal scaling law of Campi, Desbois and Lipparini.[22] This scaling law states that if one defines $X = A_{frag}/A_{tgt}$, then for a given projectile and energy, the fragment isobaric yields from all target nuclei expressed as a function of X fall on a common universal curve. Thus, in principle, one need only measure the isobaric distribution for a given projectile and energy for a single target nucleus and one will then know the distribution for all target nuclei. In Figure 8, we show the application of this idea to the fragment mass distributions from the interaction of 400 MeV/nucleon ^{20}Ne with Cu, Ho, Ta and Au. One observes some validity of the scaling law for the (Ta,Au) and (Cu, Ho) pairs but no universal scaling due to the fundamentally different shapes of the isobaric yield distributions. The (Ta,

Au) pair exhibits a U-shaped distribution not evident in the fragmentation of Cu, Ho. Perhaps a judicious application of the scaling law to extrapolate amongst smaller ranges of target nuclei is possible.

Many years ago, Rudstom parameterized the systematics of spallation yields from energetic p-nucleus collisions in a five parameter formula.[23] This semiempirical formula was extended to encompass the yields of all types of fragments from p-nucleus collisions by Silberberg and Tsao.[24] We thought it would be interesting to compare the predictions of the Silberberg-Tsao formula for p-nucleus collisions and the data for nucleus-nucleus collisions involving projectiles of equivalent total energy. (Figure 9). The magnitude (but not the shape) of the Silberberg-Tsao cross sections has been adjusted to reflect the difference between the p-nucleus and nucleus-nucleus total reaction cross sections. The agreement between the predicted and measured values of the cross sections for the Cu target nucleus is good. This agreement substantiates the oft-made claim that p-Cu and heavy ion-Cu reactions are very similar. (There is a difference between predicted and measured near-target cross sections, perhaps reflecting the influence of differing peripheral processes in p-Cu and nucleus-Cu collisions.)

When one compares predicted and measured cross sections for the Ho target nucleus, the agreement is not so good. The measured yields of fragmentation products ($A < 40$) are substantially greater in the nucleus-Ho collisions compared to the p-Ho systematics and the shapes of the mass distributions at the lower energy are not very similar . It would appear that one needs a new semi-empirical parameterization to adequately describe fragment cross sections from nucleus-nucleus collisions.

4. Semiclassical models

One of the earliest models of high energy nuclear collisions was the intranuclear cascade model. In this model, nuclear collisions are simulated by following the individual nucleon-nucleon collisions (during a reaction) using relativistic classical mechanics. The initial positions and momenta of the colliding nucleons are chosen randomly according to a prescribed distribution. For example, the momentum distribution is often chosen to be that of a cold Fermi gas. Such models traditionally ignore Pauli blocking of the nucleon-nucleon collisions, nuclear binding, etc. The single particle phase space density f (r,p,t) of the nucleons obeys a Boltzmann equation with collision terms but no mean field term.

$$\frac{\partial}{\partial t}f+\mathbf{v}\cdot\frac{\partial f}{\partial \mathbf{r}}=-\int\frac{d^3p_2 d^3p_1' d^3p_2'}{(2\pi)^6} \tag{1}$$

$$\times\ v_{12}\sigma(\mathbf{p}+\mathbf{p}_2\rightarrow\mathbf{p}_1'+\mathbf{p}_2')(ff_2-f_1'f_2')\delta^3(\mathbf{p}+\mathbf{p}_2-\mathbf{p}_1'-\mathbf{p}_2'),$$

where v_{12} is the relative velocity of the pair of particles colliding with cross section $\sigma(\mathbf{p}+\mathbf{p}_2\rightarrow\mathbf{p}_1'+\mathbf{p}_2')$. The time evolution of f (r,p,t) is followed using Monte Carlo techniques.

Our favorite version of this model is that developed by Yariv and Fraenkel.[25] Using this model, one can calculate the mass number, atomic number, excitation energy, recoil and angular momentum of the projectile and target fragments from a collision. The de-excitation of the target fragments formed in the primary interaction is calculated using yet another Monte Carlo method developed by us. In this calculation the decay of the primary fragments by evaporation and fission is followed.

In Figures 10 and 11, we compare calculations made using this semiclassical model with measured fragment mass distributions for Ho and U targets. For the case of the U target, the good agreement between the calculations and the data indicates that the de-excitation correctly describes the fission decay of the excited primary fragments. For the case of the Ho target, the agreement between the predicted and measured mass distributions is still acceptable although the measurements, particularly at the higher energy, show the occurrence of multifragmentation (yields of fragments with A<60), a phenomenon not included in the cascade model or the de-excitation calculation.

At intermediate projectile energies, many of the individual nucleon-nucleon collisions are Pauli-blocked. This can be taken into account by modifying equation (1) to include Pauli-blocking terms, i.e.,

$$\frac{\partial}{\partial t}f+\mathbf{v}\cdot\frac{\partial}{\partial \mathbf{r}}f = -\int\frac{d^3p_2 d^3p_1' d^3p_2'}{(2\pi)^6}$$

$$\times\, v_{12}\sigma\,(\mathbf{p}+\mathbf{p}_2\rightarrow\mathbf{p}_1'+\mathbf{p}_2')[ff_2(1-f_1')(1-f_2')-f_1'f_2'(1-f)(1-f_2)]$$

$$\times\,\delta^3\,(\mathbf{p}_1+\mathbf{p}_2-\mathbf{p}_1'-\mathbf{p}_2')$$

The (1-f) terms simulate the effects of Pauli blocking by inhibiting scattering to regions of high phase space density). Some success has been obtained using this model to describe the fragment mass distributions in intermediate energy nuclear reactions[17] although the lack of a mean field term in this equation does not allow a full description of all aspects of these reactions.

5. Summary

We have presented all the available data on target fragment mass distributions in intermediate and high energy nucleus-nucleus collisions. We have shown how these data may be understood in terms of semiclassical models for the reactions. We have pointed out shortcomings in various semi-empirical approaches to describing these reactions.

6. Acknowledgements

We wish to thank the many scientists who have collaborated with us in making the measurements described herein. This work was supported in part by the U.S. Dept. of Energy under contracts DE-AC03-76SF00098 and DE-AM06-76RL02227.

References

1. P.L. McGaughey, W. Loveland, D.J. Morrissey, K. Aleklett, and G.T. Seaborg, Phys. Rev. C31, 896 (1986).
2. Z. Xu, Li Wenxin, W. Loveland, P.L. McGaughey, D.J. Morrissey, R.J. Otto and G.T. Seaborg, Phys. Rev. C (in preparation).
3. W. Loveland, K. Aleklett, P.L. McGaughey, K.J. Moody, R.M. McFarland, R.H. Kraus, Jr., and G.T. Seaborg, Lawrence Berkeley Laboratory Report LBL-16280, July, 1983.
4. H. Kudo, K.J. Moody, and G.T. Seaborg, Phys. Rev. C30, 1561 (1984).
5. K. Aleklett, W. Loveland, C. Casey, J.O. Liljenzin, D.J. Morrissey, M. de Saint Simon, G.T. Seaborg, and L. Sihver, Nucl. Phys. A (in preparation).
6. D.J. Morrissey, W. Loveland, M. de Saint Simon, and G.T. Seaborg, Phys. Rev. C21, 1783 (1980).

7. S.B. Kaufman, E.P. Steinberg, B.D. Wilkins and D.J. Henderson, Phys. Rev. C22, 1897 (1980).

8. W. Loveland, K. Aleklett, M. Bronikowski, Y.Y. Chu, J.B. Cumming, P.E. Haustein, S. Katcoff, N.T. Porile and L. Sihver, Phys. Rev. C (in preparation).

9. R. Kraus, Ph.D. thesis, Oregon State University, 1986 (unpublished).

10. S.Y. Cho, Y.H. Chung and N.T. Porile, Phys. Rev. C (submitted for publication).

11. T. Lund, D. Molzahn, R. Brandt, B. Bergersen, D. Eriksen, E. Hagebø, I.R. Haldorsen, T. Bjornstad, and C. Richard-Serre, Phys. Lett. 10213, 239 (1981).

12. K.E. Hicks, T.E. Ward, H. Bowman, J.G. Ingersoll, J.D. Rasmussen, J.P. Sullivan, M. Loike and J. Peter, Phys. Rev. C26, 2016 (1982).

13. J.B. Cumming, P.E. Haustein, R.W. Stoenner, L. Mausner and R.A. Naumann, Phys. Rev. C10, 739 (1974).

14. J.B. Cumming, R.W. Stoenner, and P.E. Haustein, Phys. Rev. C14, 1554 (1976).

15. A. Lleres, J. Blachot, J. Crancon, A. Gizon, and H. Nifenecker, Z. Phys. A312, 177 (1983).

16. N.T. Porile, G.D. Cole and C.R. Rudy, Phys. Rev. C19, 2288 (1979).

17. K. Aleklett, W. Loveland, T.T. Sugihara, A.N. Behkami, D.J. Morrissey, Li Wenxin, Wing Kot, and G.T. Seaborg, Phys. Scr. 34, 489 (1986).

18. W. Loveland, C.P. Oertel, D.J. Morrissey, P.L. McGaughey, G.T. Seaborg and K. Aleklett, LBL-16931.

19. W. Loveland, Cheng Luo, P.L. McGaughey, D.J. Morrissey and G.T. Seaborg Phys. Rev. C24, 464 (1981).

20. K. Aleklett, W. Loveland, L. Sihver, Z. Xu, C. Casey, and D. J. Morrissey, J.O. Liljenzin, M. De Saint-Simon and G.T. Seaborg, Phys. Rev. C (in preparation).

21. W. Loveland, K. Aleklett and G.T. Seaborg. Nucl. Phys. A447, 101 (1985).

22. X. Campi, J. Desbois and E. Lipparini, Phys. Lett 138B, 353 (1984).

23. G. Rudstam, Z. Naturforschung 21a, 1027 (1966).

24. R. Silberberg and C.H. Tsao, Astrphys. J. Suppl. Ser. 220, 25, 315 (1973); 25, 335 (1973).

25. Y. Yariv and Z. Fraenkel, Phys. Rev. C20, 2227 (1979).

Figure Captions

Figure 1. Fragment mass distributions for the reaction of 1.0, 3.0, 4.8, 12 and 25 GeV ^{12}C with ^{238}U. The data for the first four energies are from Ref. 1, the 25 GeV data are from Ref. 2.

Figure 2. Left panels - Fragment mass yield distributions for the reaction of 8.0 and 20 GeV ^{20}Ne with ^{238}U (Ref. 1). Right panels-Comparison of mass yield curves for the ^{12}C and ^{20}Ne induced reactions. For the ^{12}C + ^{238}U reactions, the solid, dotted, dashed and dash-dotted curves represent reactions induced by 1.0, 3.0, 4.8 and 12 GeV, respectively. For the ^{20}Ne + ^{238}U reactions, the dotted and dashed curves represent projectile energies of 8.0 and 20 GeV, respectively.

Figure 3. Fragment mass distributions for the fragmentation of ^{197}Au by 12 MeV/nucleon O^{16} (Ref. 3), 18.4 MeV/nucleon ^{16}O (Ref. 3), 20 MeV/nucleon ^{12}C (Ref. 4), 35 MeV/nucleon (Ref. 5), 45.4 MeV/nucleon ^{12}C (Ref. 3.) and 83.8 MeV/nucleon ^{12}C (Ref. 3.)

Figure 4. Fragment mass distributions for the fragmentation of ^{197}Au by 400 MeV/nucleon ^{20}Ne (Ref. 6), 400 MeV/nucleon ^{12}C (ref. 7) and 14.6 GeV/nucleon ^{16}O (ref. 8.)

Figure 5. Fragmentation of ^{165}Ho by intermediate energy heavy ions. From Ref. 9.

Figure 6. Fragmentation of ^{165}Ho by relativistic heavy ions. From Ref. 9.

Figure 7. Fragmentation of Cu by 35 MeV/nucleon ^{12}C (Ref. 10), 86 MeV/nucleon ^{12}C (Ref. 11), 211 MeV/nucleon ^{20}Ne (ref. 12), 279 MeV/nucleon ^{14}N (Ref. 13), 377 MeV/nucleon ^{20}Ne (Ref. 12) and 2.1 GeV/nucleon ^{12}C (Ref. 14).

Figure 8. Fragment isobaric yield distributions for the interaction of 400 MeV/nucleon ^{20}Ne with Cu (solid circles, Ref. 12), Ho (open circles, Ref. 9), Ta (solid line, Ref. 6) and Au (dotted line, Ref. 6) as a function of the scaling parameter X.

Figure 9. Comparisons of the predictions of the Silberberg-Tsao formula (solid line) with the measured fragment mass distributions (solid points) for the interaction of 279 MeV/A ^{14}N and 2.1 GeV/A ^{12}C with Cu and 3 and 12 GeV ^{12}C with ^{165}Ho.

Figure 10. Comparison of measured (solid points) and predicted (cascade, histogram) fragment mass distributions for Ho targets.

Figure 11. Comparison of measured (solid line) and predicted (cascade, solid histogram) U target fragment mass distributions. (The dashed histogram represents the predictions of the nuclear firestreak model[1])

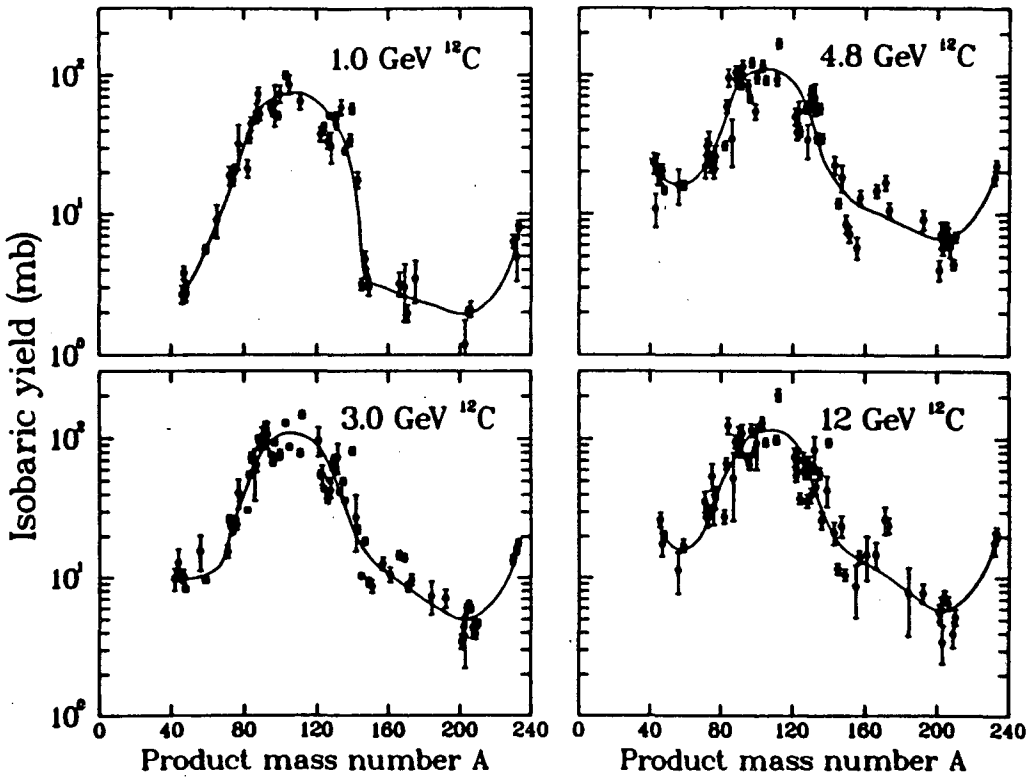
1.0 GeV ^{12}C
4.8 GeV ^{12}C
3.0 GeV ^{12}C
12 GeV ^{12}C
Isobaric yield (mb)
Product mass number A
Product mass number A

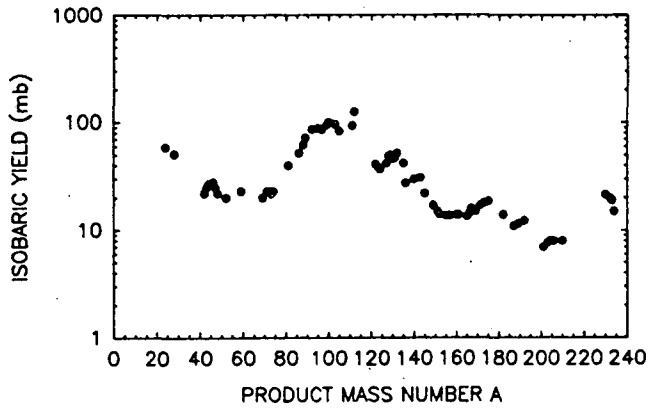
ISOBARIC YIELD (mb)
PRODUCT MASS NUMBER A

Fig. 1

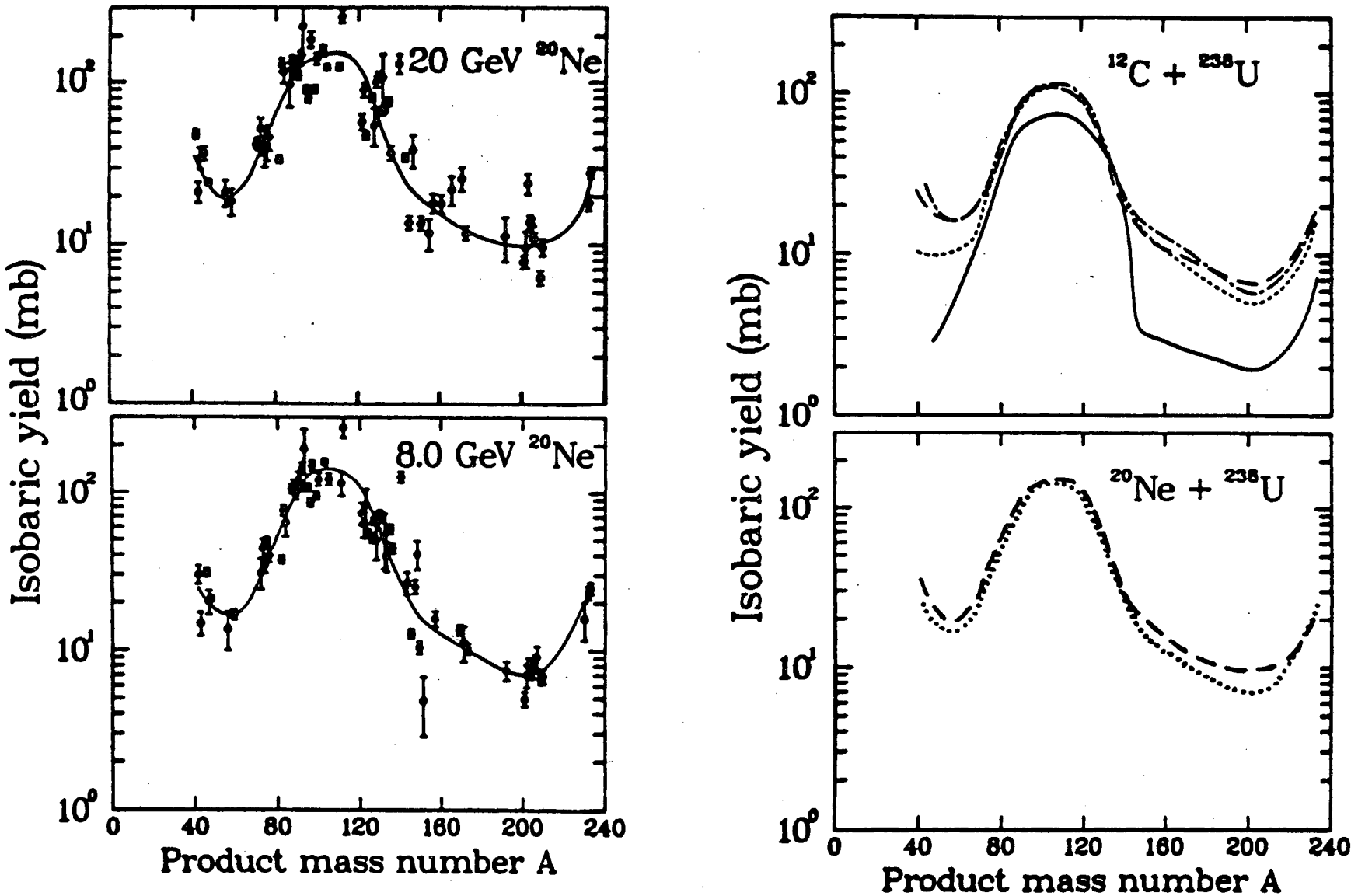
20 GeV ^{20}Ne
8.0 GeV ^{20}Ne
^{12}C + ^{238}U
^{20}Ne + ^{238}U
Isobaric yield (mb)
Product mass number A
10^0
10^1
10^2
0
40
80
120
160
200
240

Fig. 2

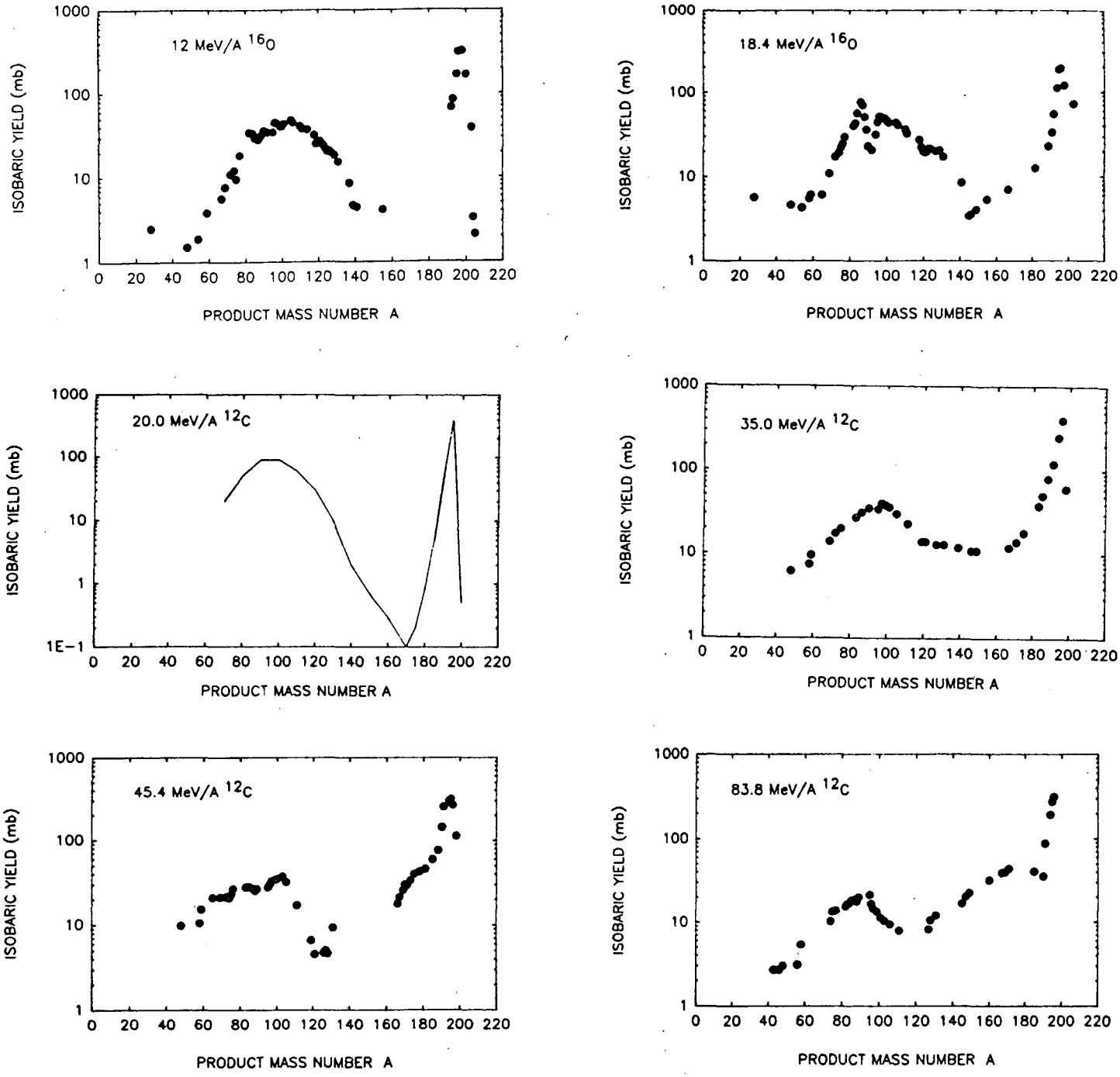
12 MeV/A 16O
18.4 MeV/A 16O
20.0 MeV/A 12C
35.0 MeV/A 12C
45.4 MeV/A 12C
83.8 MeV/A 12C
ISOBARIC YIELD (mb)
PRODUCT MASS NUMBER A
1000
100
10
1
1E-1
0 20 40 60 80 100 120 140 160 180 200 220

Fig. 3

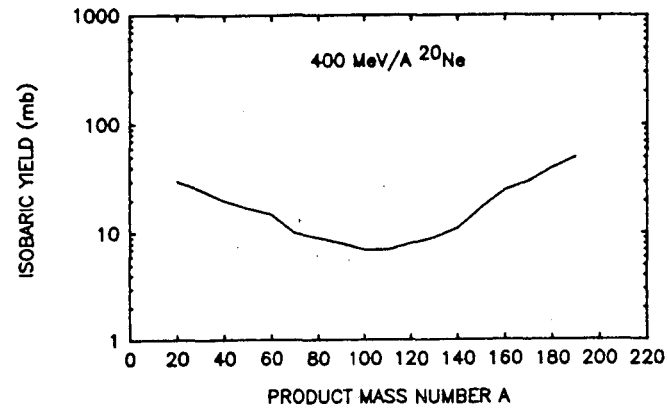
400 MeV/A ^{20}Ne
ISOBARIC YIELD (mb)
1000
100
10
1
0 20 40 60 80 100 120 140 160 180 200 220
PRODUCT MASS NUMBER A

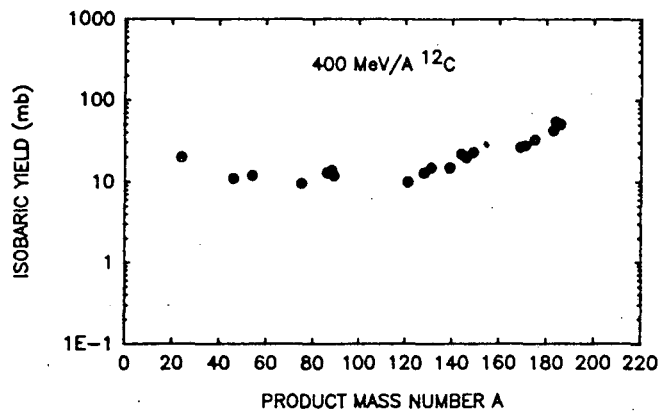
400 MeV/A ^{12}C
ISOBARIC YIELD (mb)
1000
100
10
1
1E−1
0 20 40 60 80 100 120 140 160 180 200 220
PRODUCT MASS NUMBER A

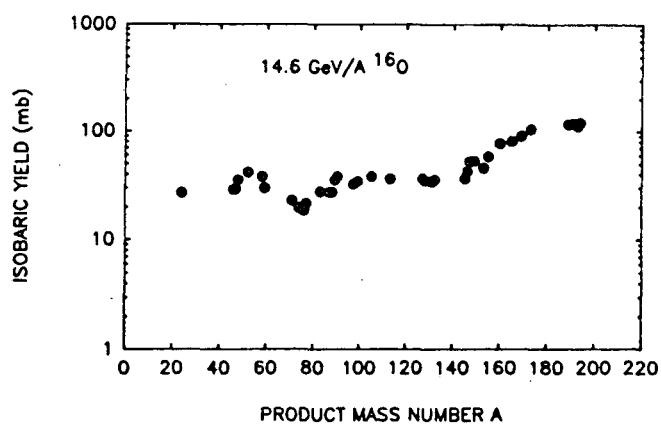
14.6 GeV/A ^{16}O
ISOBARIC YIELD (mb)
1000
100
10
1
0 20 40 60 80 100 120 140 160 180 200 220
PRODUCT MASS NUMBER A

Fig. 4

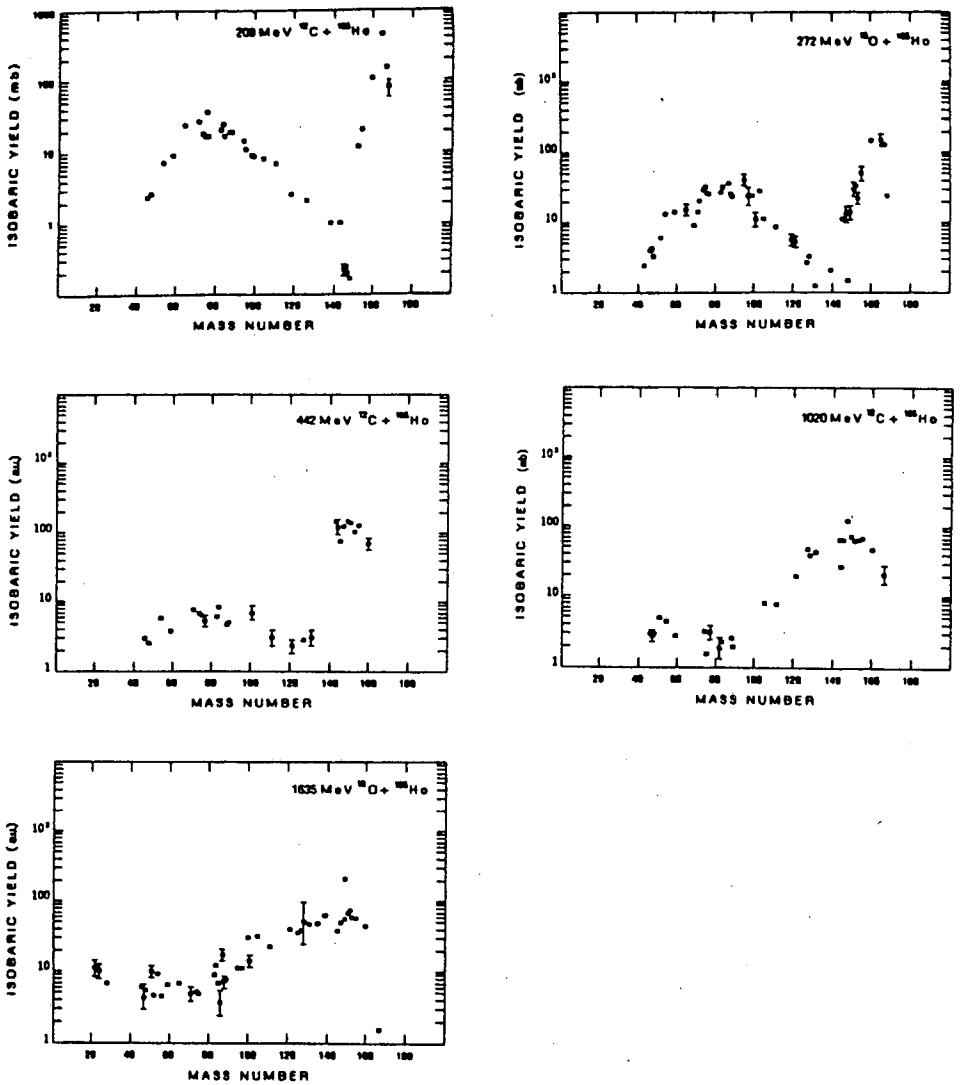
208 MeV 12C + 165Ho
272 MeV 16O + 165Ho
442 MeV 12C + 165Ho
1020 MeV 12C + 165Ho
1635 MeV 16O + 165Ho
ISOBARIC YIELD (mb)
MASS NUMBER

Fig. 5

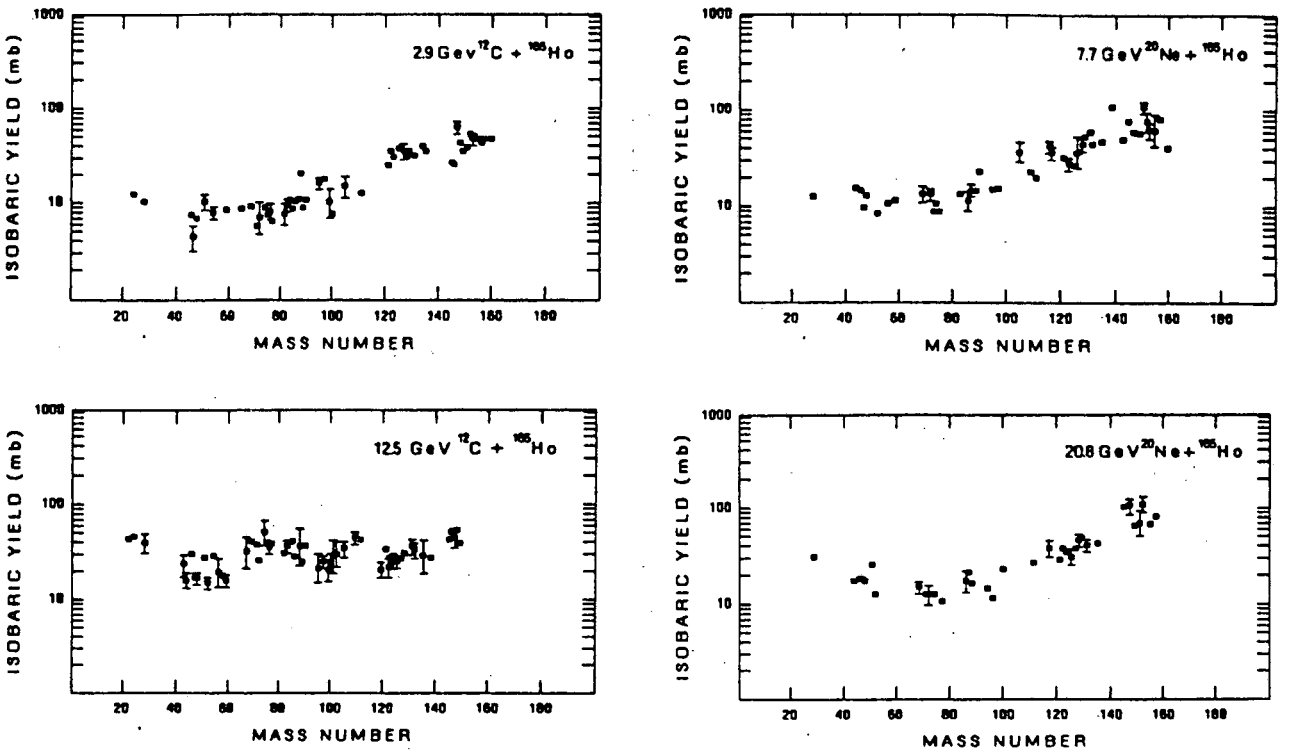
2.9 GeV ^{12}C + ^{165}Ho
7.7 GeV ^{20}Ne + ^{165}Ho
12.5 GeV ^{12}C + ^{165}Ho
20.8 GeV ^{20}Ne + ^{165}Ho
ISOBARIC YIELD (mb)
MASS NUMBER
1000
100
10
20
40
60
80
100
120
140
160
180

Fig. 6

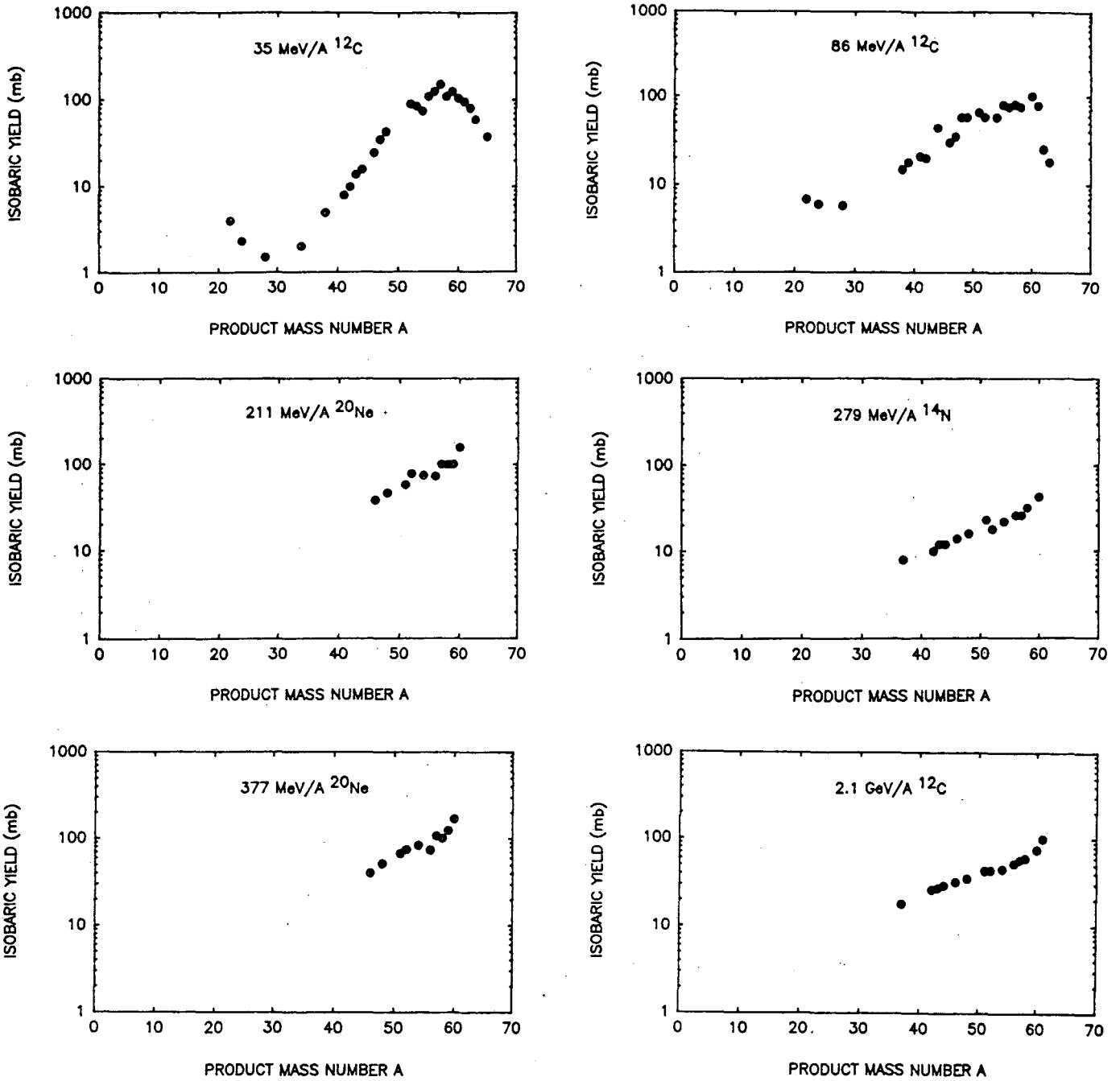
35 MeV/A 12C
86 MeV/A 12C
211 MeV/A 20Ne
279 MeV/A 14N
377 MeV/A 20Ne
2.1 GeV/A 12C
ISOBARIC YIELD (mb)
PRODUCT MASS NUMBER A
1000
100
10
1
0
10
20
30
40
50
60
70

Fig. 7

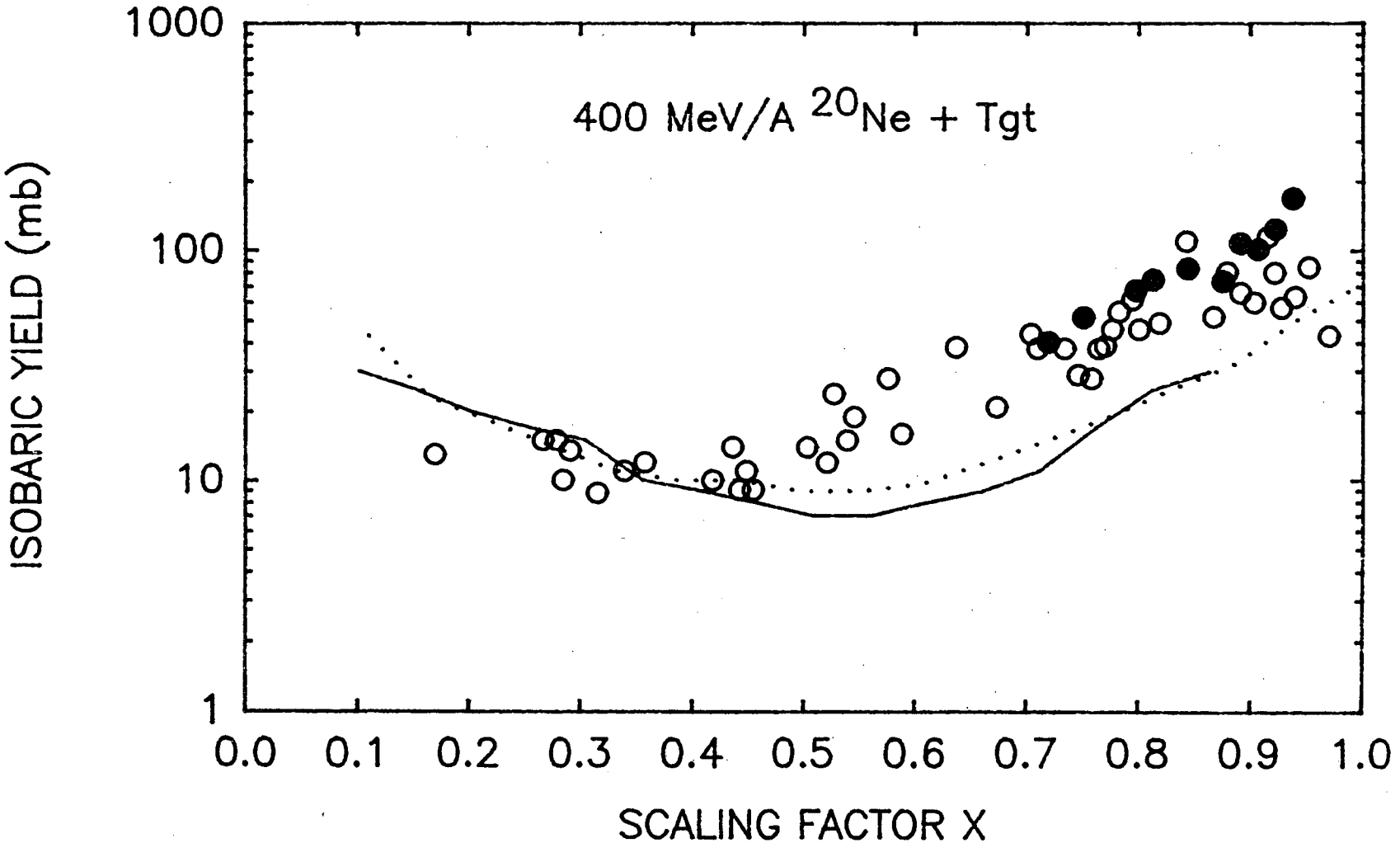
400 MeV/A ^{20}Ne + Tgt
ISOBARIC YIELD (mb)
1000
100
10
1
0.0
0.1
0.2
0.3
0.4
0.5
0.6
0.7
0.8
0.9
1.0
SCALING FACTOR X

Fig. 8

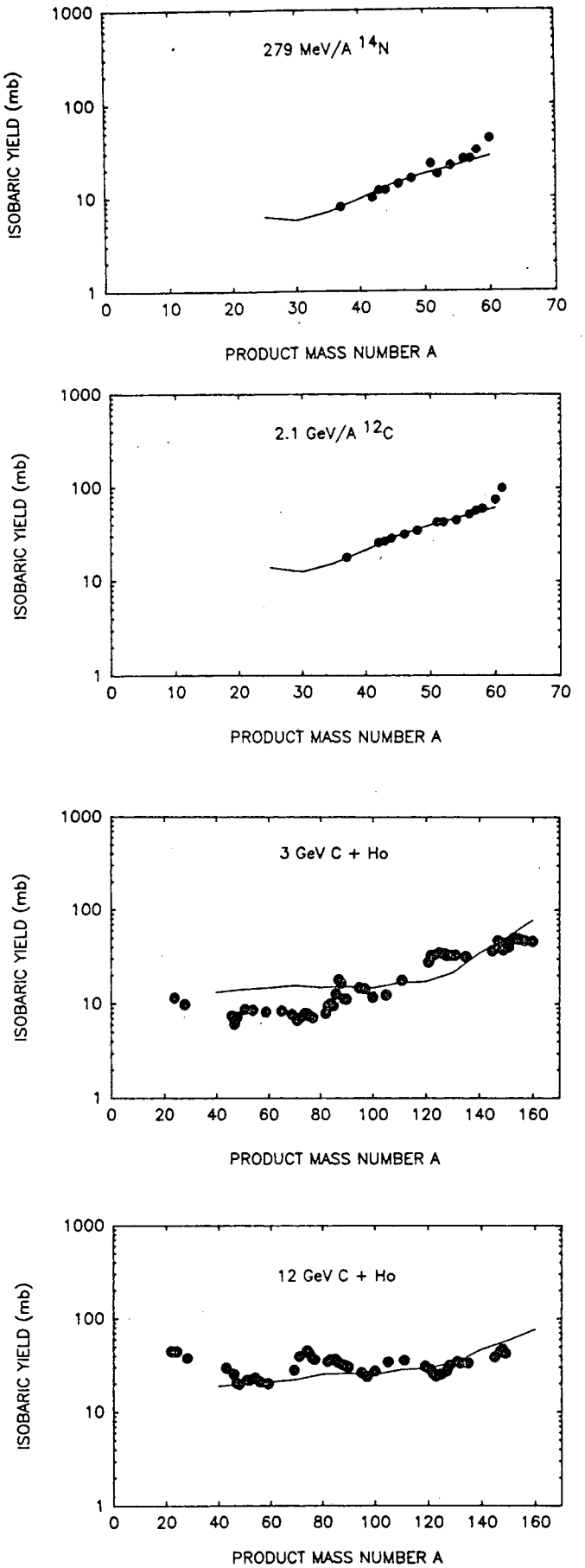
279 MeV/A ^{14}N
2.1 GeV/A ^{12}C
3 GeV C + Ho
12 GeV C + Ho
ISOBARIC YIELD (mb)
PRODUCT MASS NUMBER A
1000
100
10
1
0
10
20
30
40
50
60
70
80
100
120
140
160

Fig. 9

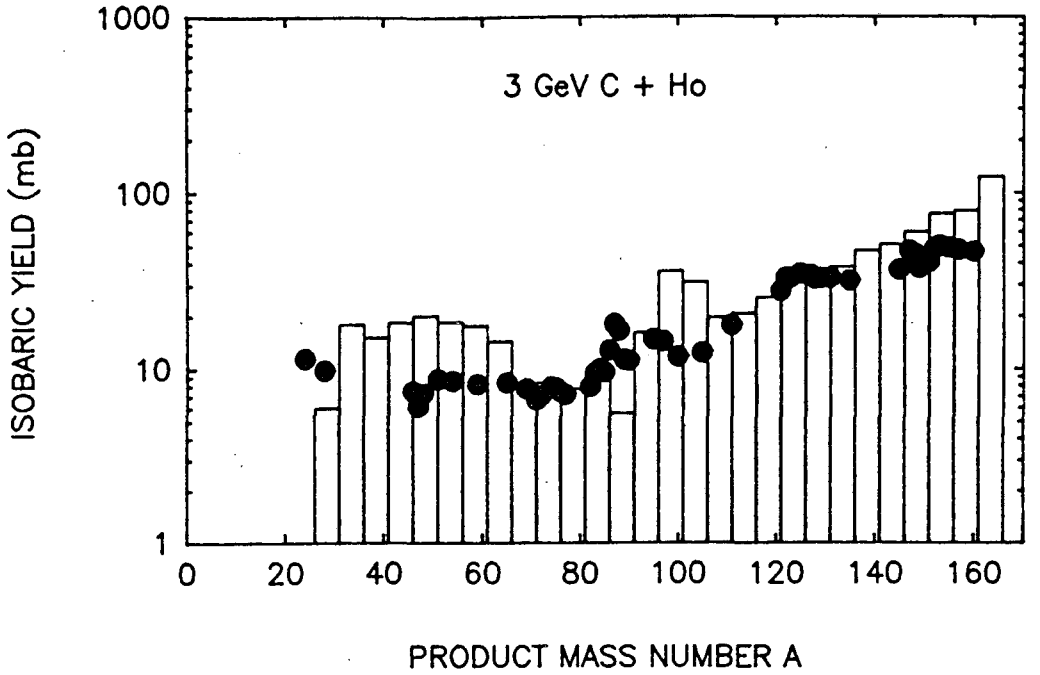
3 GeV C + Ho
ISOBARIC YIELD (mb)
1000
100
10
1
0
20
40
60
80
100
120
140
160
PRODUCT MASS NUMBER A

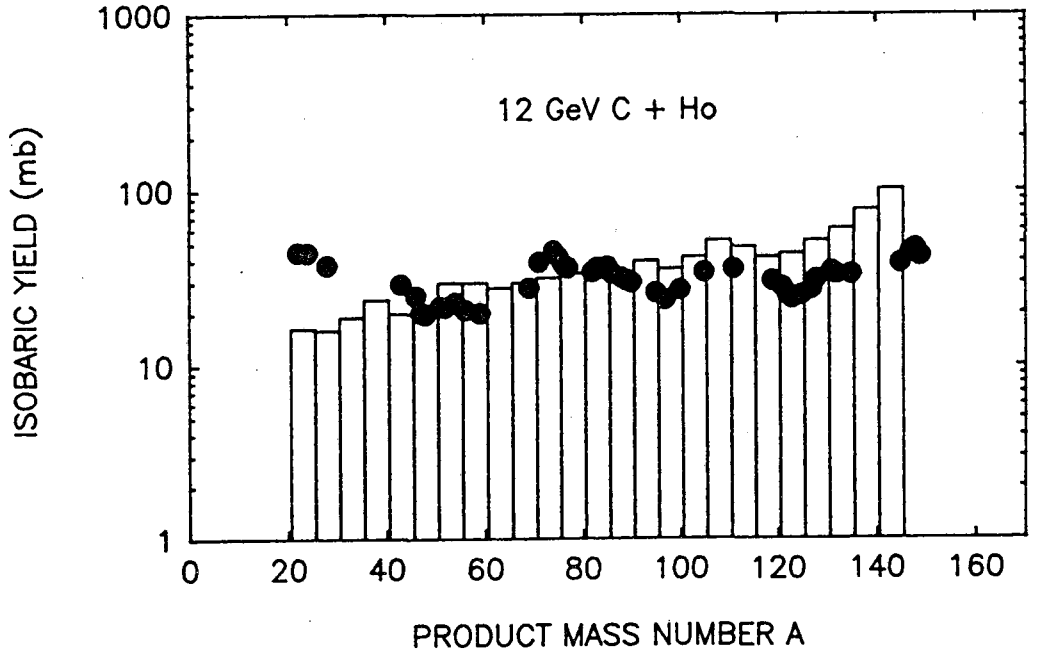
12 GeV C + Ho
ISOBARIC YIELD (mb)
1000
100
10
1
0
20
40
60
80
100
120
140
160
PRODUCT MASS NUMBER A

Fig. 10

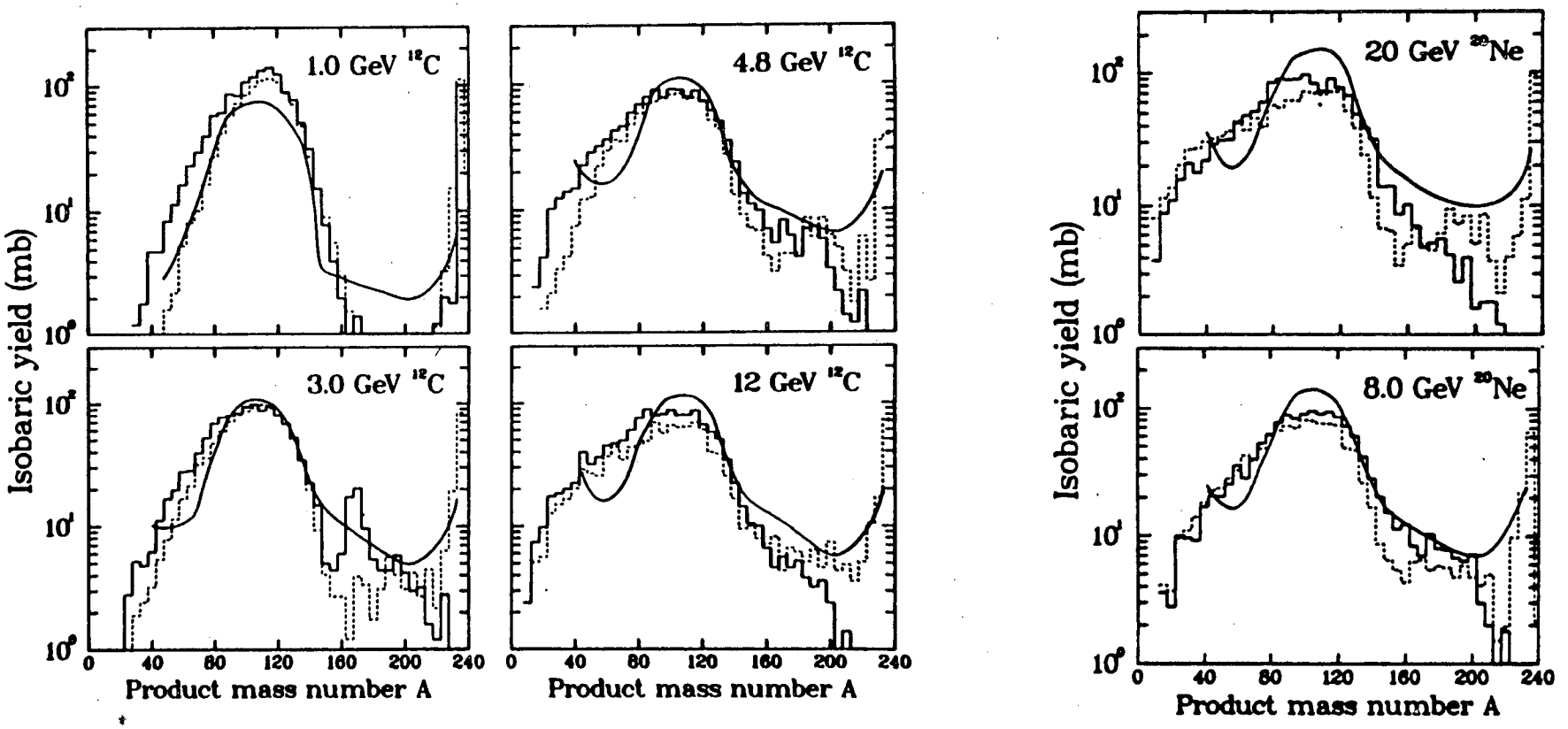
1.0 GeV ^{12}C
4.8 GeV ^{12}C
3.0 GeV ^{12}C
12 GeV ^{12}C
20 GeV ^{20}Ne
8.0 GeV ^{20}Ne
Isobaric yield (mb)
Product mass number A
0
40
80
120
160
200
240

Fig. 11

LAWRENCE BERKELEY LABORATORY
TECHNICAL INFORMATION DEPARTMENT
UNIVERSITY OF CALIFORNIA
BERKELEY, CALIFORNIA 94720